


Article

Drug Responses in Plexiform Neurofibroma Type I (PNF1) Cell Lines Using High-Throughput Data and Combined Effectiveness and Potency

Paul O. Zamora¹, Gabriel Altay², Ulisses Santamaria³, Nathan Dwarshuis¹, Hari Donthi¹, Chang In Moon^{4,5}, Dana Bakalar⁶ and Matthew Zamora^{1,*} 

¹ MoCo Makers, Gaithersburg, MD 20879, USA

² HacDC, Washington, DC 20010, USA

³ DMV Petri Dish, Rockville, MD 20850, USA; ulisses@dmvpetridish.com

⁴ Dan L. Duncan Comprehensive Cancer Center, Department of Molecular and Human Genetics, Baylor College of Medicine, Houston, TX 77030, USA

⁵ Lester and Sue Smith Breast Center, Department of Molecular and Human Genetics, Baylor College of Medicine, Houston, TX 77030, USA

⁶ National Institute of Neurological Diseases and Stroke, National Institutes of Health, Bethesda, MD 20892, USA

* Correspondence: matt@mocomakers.com

Simple Summary: Neurofibromatosis 1 (NF1) is a genetic disorder that predisposes patients to developing nerve sheath tumors that are difficult to treat. There is currently just one drug approved for the treatment of NF1-related inoperable plexiform neurofibromas (for a limited patient population), highlighting the need for further drug discovery in this field. High-throughput screening data are used to guide drug development, but identifying and selecting promising targets can be complex. The aim of our study is to improve the value of high-throughput screening data by combining potency and effectiveness into single-value indices (S , ΔS , and ΔS mean), which are used to assess and rank drug sensitivity and drug resistance in cells exposed to potential therapeutic drugs. Our approach with S indices was applied to cell lines derived from plexiform neurofibromas of patients with $NF1$ gene mutations. The use of S indices provides valuable additional and independent information for discriminating among candidate compounds for follow-up pre-clinical evaluations.

Abstract: *Background:* Neurofibromatosis type 1 (NF1) is a genetic disorder characterized by heterozygous germline $NF1$ gene mutations that predispose patients to developing plexiform neurofibromas, which are benign but often disfiguring tumors of the peripheral nerve sheath induced by loss of heterozygosity at the $NF1$ locus. These can progress to malignant peripheral nerve sheath tumors (MPNSTs). There are no approved drug treatments for adults with NF1-related inoperable plexiform neurofibromas, and only one drug (selumetinib), which is an FDA-approved targeted therapy for the treatment of symptomatic pediatric plexiform neurofibromas, highlighting the need for additional drug screening and development. In high-throughput screening, the effectiveness of drugs against cell lines is often assessed by measuring in vitro potency (AC50) or the area under the curve (AUC). However, the variability of dose–response curves across drugs and cell lines and the frequency of partial effectiveness suggest that these measures alone fail to provide a full picture of overall efficacy. *Methods:* Using concentration–response data, we combined response effectiveness (EFF) and potency (AC50) into (a) a score characterizing the effect of a compound on a single cell line, $S = \log[\text{EFF}/\text{AC50}]$, and (b) a relative score, ΔS , characterizing the relative difference between a reference (e.g., non-tumor) and test (tumor) cell line. ΔS was applied to data from high-throughput screening (HTS) of a drug panel tested on $NF1$ –/– tumor cells, using immortalized non-tumor $NF1$ +/– cells as a reference. *Results:* We identified drugs with sensitivity, targeting expected pathways, such as MAPK-ERK and PI3K-AKT, as well as serotonin-related targets, among others. The ΔS technique used here, in tandem with a supplemental ΔS web tool, simplifies HTS analysis and may provide a springboard for further investigations into drug response in NF1-related cancers. The tool may also prove useful for drug development in a variety of other cancers.



Citation: Zamora, P.O.; Altay, G.; Santamaria, U.; Dwarshuis, N.; Donthi, H.; Moon, C.I.; Bakalar, D.; Zamora, M. Drug Responses in Plexiform Neurofibroma Type I (PNF1) Cell Lines Using High-Throughput Data and Combined Effectiveness and Potency. *Cancers* **2023**, *15*, 5811. <https://doi.org/10.3390/cancers15245811>

Academic Editors: Daochun Sun and Sameer Farouk Sait

Received: 21 November 2023

Revised: 5 December 2023

Accepted: 8 December 2023

Published: 12 December 2023



Copyright: © 2023 by the authors. Licensee MDPI, Basel, Switzerland. This article is an open access article distributed under the terms and conditions of the Creative Commons Attribution (CC BY) license (<https://creativecommons.org/licenses/by/4.0/>).

Keywords: neurofibromatosis; NF1; high-throughput; plexiform; drug evaluation; in vitro; concentration–response; web tool

1. Introduction

Neurofibromatosis type 1 (NF1) is a rare chronic neurocutaneous disease caused by loss-of-function alterations in the gene *NF1*, encoding the tumor suppressor neurofibromin [1,2]. Via RAS inhibition, *NF1* mutations affect multiple signaling pathways linked to cell survival and proliferation and the development of cancers. NF1 patients often develop neurofibromas, which are benign peripheral nerve sheath tumors. In 8% to 16% of NF1 patients, however, these benign neurofibromas progress to malignant peripheral nerve sheath tumors (MPNSTs) [3,4]. MPNSTs are characterized by the deletion or loss of function of tumor suppressors, including neurofibromin itself, and amplifications or gain of function mutations in several oncogenes, including *MET*, *EGFR*, and other receptor tyrosine kinases. Other deregulated pathways in MPNSTs include the MTOR, HIPPO, WNT, and RAS signaling pathways [5].

Currently, the sole FDA-approved drug treatment for NF1-associated inoperable plexiform neurofibromas is the MEK inhibitor selumetinib [6–8], which is indicated for the treatment of pediatric (but not adult) NF1-associated nerve sheath tumors. This deficit highlights the need for different ways to derive promising targets and new drugs.

One drug development technique involves using high-throughput screening (HTS) to assess the effect of an array of drugs on cancer cells and, thereby, identify promising targets for further experimentation. The effective prioritization of drugs depends on the appropriate analysis of the resulting data. Typically, the prioritization of drugs has been quantified through evaluating AC50, or area under the curve (AUC) values. Both techniques have limitations. AC50 is the concentration of a drug that induces half-maximal activity. The relative potency of two compounds can be compared by computing the log of the ratio of two AC50 values ($\Delta pAC50$). For drugs generating complete cytotoxic responses within a given concentration range, AC50 and $\Delta pAC50$ values can effectively be used for comparison. This relationship breaks down, however, when one or both of the drugs being compared are only partially effective, which is a common finding in HTS [9–11].

The AUC is the area under the response curve for a cell population over the tested drug concentration range. There are, however, reports of poor concordance of half-maximal inhibitory concentration (IC50) and AUC measures [12] (as well as AC50 and AUC). Guha et al. [13] have also pointed out additional issues involving the use of AUC, which may limit its general utility.

To address these limitations, we developed relative activity scales (*S* indices) for normalizing and measuring drug activity. The *S*-index combines potency and effectiveness data, facilitating a comparison of the relative activity of compounds across drug classes and cell lines. Normalizing activity by including the maximal response corrects for differences in full or partial drug sensitivity and can be determined without the need to re-fit the underlying concentration–response data to a more complex model [14]. We applied our *S*-index analysis to a high-throughput screening dataset [15], which screened a panel of 1912 drugs against NF1-patient-derived neurofibroma cell lines and reference peripheral nerve cell lines (see Table 1). The resulting list of drugs to which these cell lines are sensitive or resistant, and the algorithm itself, may prove useful in drug development efforts.

Table 1. Description of immortalized human cell lines used in the study.

Human Cell Lines			
Cell Line	Immortalized	Tissue Source	Neurofibromin Status
ipnNF95.11C *	yes	Peripheral nerve (non-tumor)	+/-
ipNF06.2A	yes	Plexiform Neurofibroma (PNF1)	-/-
ipNF95.6 *	yes	Plexiform Neurofibroma (PNF1)	-/-
ipNF95.11b C/T	yes	Plexiform Neurofibroma (PNF1)	-/-
ipNF05.5 Mixed Clone (ipNF05.5-MX)	yes	Plexiform Neurofibroma (PNF1)	-/-

* A recent analysis (M.R. Wallace, personal communication) has suggested that the cell lines ipnNF95.11C and ipNF95.6 may consist of a mixed population of homozygous *NF1*^{-/-} and heterozygous *NF1*^{+/-} cells, although the initial testing [15,16] reported them as in the table above and we analyzed them as such.

2. Materials and Methods

2.1. Cell Lines, Data Access, and Extraction

To assess our analysis algorithm and identify promising targets, we analyzed an HTS dataset produced by Ferrer et al. [15], which reported pharmacologic and genomic profiling of plexiform neurofibroma-derived Schwann cells from *NF1* patients and control nerve cells. Proliferation assays were used to screen a panel of 1912 small molecules (the MIPE 4.0 library [17]) against immortalized *NF1*^{-/-}, *NF1*^{+/-}, and *NF1*^{+/+} cell lines [16], with the fluorescence intensity indicating survival and proliferation after treatment.

Primary files [15] were accessed from Single Agent Screens through Synapse <https://doi.org/10.7303/syn4939906> (accessed on 1 May 2023). Access was provided by the Children’s Tumor Foundation through their 2022 Hack4NF project.

The following data were extracted from primary files: cell line name, drug name and target, log AC50 (LAC50, i.e., the log of the active concentration for a half-maximal response in molar concentration), R2 (R², goodness of fit for the 4-parameter logistic regression model) values of dose–response curves, AUC (TAUC, total area under the curve), the asymptote minimum (“INF”, response extrapolated to infinite concentration), and the asymptote maximum (“ZERO”, response extrapolated to zero concentration).

Separately, response data (dat0–dat10) and concentration (C0–C10, in μM) were downloaded and analyzed using a 4-parameter fit in SigmaPlot and with the DREA web tool (see Supplemental Materials). The DREA web tool recreates our final compound rankings using the application’s default filters, based on the data files from Ferrer et al. [15].

2.2. Data Analysis

2.2.1. AC50 (Potency) and Relative Potency

The log AC50 values (in M) were converted to AC50 (in μM), which is a commonly used potency measure. The relative potency ($\Delta pAC50$) of a compound exposed to two cell lines is defined in Equations (1) and (2). For the data presented in the Results section, the reference (*ref*) cell line was ipnNF95.11C (note that other reference lines can be selected—see our discussion on multiple controls) and the test (*test*) was one of the PNF1 cell lines. Generally, $\Delta AC50 > 0$ indicates that the test cell lines were more sensitive to a compound than the reference cell line.

$$\Delta AC50 = \left[\log AC50_{ref} - \log AC50_{test} \right] = \log \left[\frac{AC50_{ref}}{AC50_{test}} \right] \quad (1)$$

$$\Delta pAC50 = - \left[\log AC50_{ref} - \log AC50_{test} \right] = - \log \left[\frac{AC50_{ref}}{AC50_{test}} \right] \quad (2)$$

In an analogous manner, the AUC, as provided in the original dataset (TAUC, total AUC), was used to determine the relative AUC ($\Delta pAUC50$) using a method analogous to

those described in Equations (1) and (2), except that the appropriate AUC values were used (in place of AC50). As described above, the reference cell line was ipnNF95.11C and the test was one of the PNF1 cell lines.

2.2.2. The S and ΔS Indices

We establish an algorithm for creating a single value score ΔS , which compares the relative effect of a given compound between a test cell line and a reference cell line. This is, in turn, generated from S , which incorporates both AC50 (potency) and the effectiveness into a single value for a single compound in a single cell line. Equation (3) defines effectiveness (EFF) from concentration–response curves and is calculated as the response asymptote at the maximum dose concentration (ASM_{Max}) minus the response asymptote at the minimum dose concentration (ASM_{Min}). These two values (EFF and AC50) were incorporated into a single value S , reflecting both effectiveness and potency (Equation (4)) and, therefore, the overall response for a single compound in a single cell line. The relative value ΔS assesses change in S from a reference cell line (S_{ref}) to S from a test cell line (S_{test}); that is to say ($S_{ref} - S_{test}$) (Equation (5)).

$$EFF = ASM_{Max} - ASM_{Min} \quad (3)$$

$$S = \log\left(\frac{EFF}{AC50}\right) \quad (4)$$

$$\Delta S = S_{ref} - S_{test} = \log\left(\frac{EFF}{AC50}\right)_{ref} - \log\left(\frac{EFF}{AC50}\right)_{test} = \log\left[\left(\frac{EFF_{ref}}{EFF_{test}}\right)\left(\frac{AC50_{test}}{AC50_{ref}}\right)\right] \quad (5)$$

The ΔS value can be envisioned as a theoretical log molar ratio where both the reference and test are compared in a way that both reports complete responses and correct for partial responses based on the input data. The test response is normalized, relative to the reference. Note that the magnitude of S depends on the units of response and concentration, but ΔS is a unitless quantity. This approach is analogous to that described by others and used in receptor pharmacology [10,14,18].

The ΔS score was used to monitor the relative effects of compounds across cell lines and monitor the effects of several compounds in a single cell line. When the compound resulted in a higher ΔS in the reference cell line than in the test cell line, the test cell line was considered resistant to the compound.

$$\text{Drug resistant, } \Delta S = (S_{ref} - S_{test}) > 0 \quad (6)$$

When the compound gave a lower ΔS in the reference cell line than in the test cell line, the test cell line was considered sensitive to the compound.

$$\text{Drug sensitive, } \Delta S = (S_{ref} - S_{test}) < 0 \quad (7)$$

Since the tumor cell lines could have different drug sensitivities and harbor mutations that impact different intracellular signaling pathways and processes, we ranked compounds with ΔS for individual cell lines. Then a consolidated evaluation of cell lines was established as the ΔS mean, which is a simple mean of the ΔS values for a compound across the PNF1 cell lines.

2.2.3. Prioritization

To further prioritize compounds for a more in-depth follow-up, we selected compounds that generated concentration–response curves with an average R^2 of at least 0.8 in all four test cell lines. R^2 values from the reference cell line were similarly set to at least 0.8, and compounds that did not meet this threshold were excluded from the prioritized list, except for cases where there was no concentration–response. For the com-

pounds meeting prioritization criteria, the ΔS mean and ΔS variance of the mean were calculated. Compounds displaying drug resistance (ΔS mean > 0.5) or drug sensitivity (ΔS mean < -0.5) were considered potentially biologically meaningful, as they would represent approximately a 3-fold change on an arithmetic scale (Figure 1). An additional threshold of 0.3 was set for the lower boundary of variance of the mean to ensure that the mean values were at least non-inferior to a null response. Non-inferiority can be shown if the difference between the two treatments does not cross a predefined inferiority margin. A threshold of 0.3 would represent approximately a 2-fold difference in an arithmetic scale.

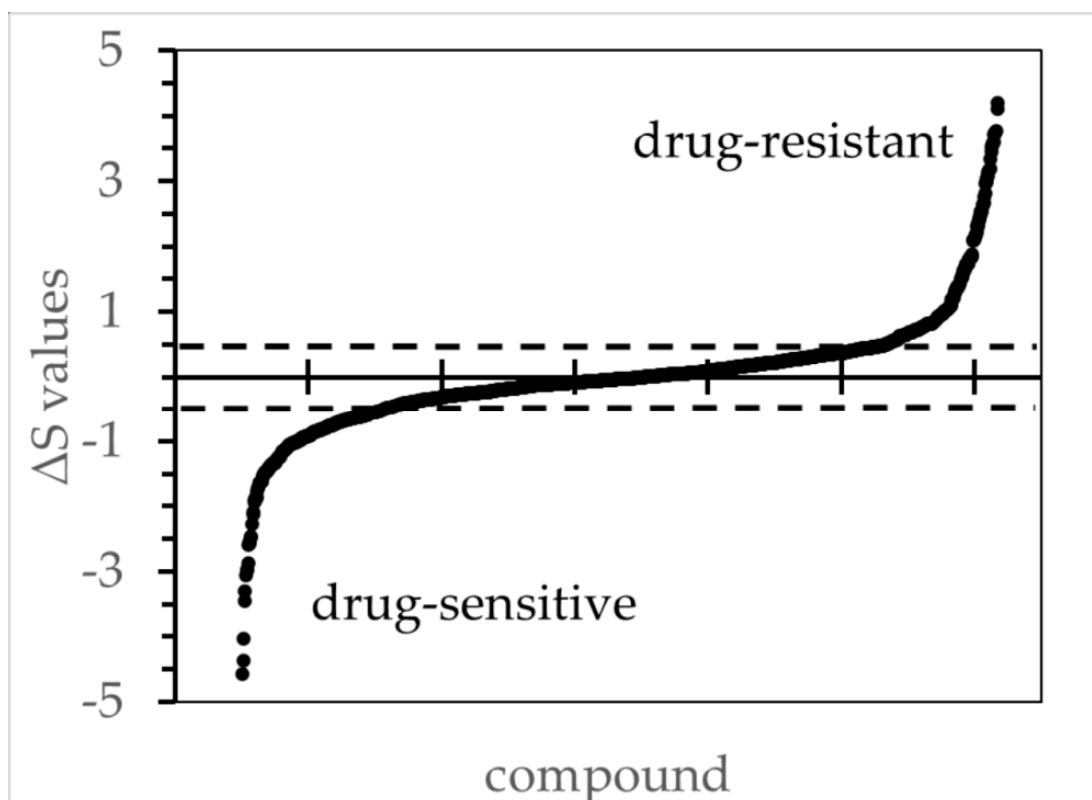


Figure 1. The ΔS values for all tested compounds comparing ipNF95.6 against the reference cell line ipnNF95.11C. The figure illustrates the order of ΔS values from low to high based on concentration/response curves, wherein the R^2 values were ≥ 0.8 . The ΔS thresholds 0.5 and -0.5 are marked with a dotted line, and values beyond those were deemed to be biologically significant during the subsequent candidate selection. Other PNF1 cell lines had similar distributions (not shown).

2.2.4. Reference Cell Line and Use of Alternate and Multiple Controls

For our analysis, we primarily used the $NF1+/-$ cell line ipnNF95.11C as our reference cell line and the $NF1-/-$ plexiform neurofibroma cell lines (PNF1 cells) ipNF05.5-MX, ipNF06.2A, ipNF95.11b C/T, and ipNF95.6 as test lines. The reference ipnNF95.11C cell line is derived from the non-tumor peripheral nerve of an $NF1$ patient and was selected because individuals with $NF1$ syndrome have a constitutional heterozygosity for $NF1$. Neurofibromas often arise from cells with additional somatic mutations of $NF1$ [14]. Ideal therapies would, therefore, target $NF1-/-$ neurofibroma cells, but not background $NF1+/-$ cells to yield maximum anti-tumor specificity.

The dataset from Ferrer et. al. also included additional neurofibromin-competent cell lines, specifically human foreskin fibroblasts [HFF] and the Schwann cell lines ipNF02.3 2λ , ipNF02.8. ΔS calculations using these other control lines can be investigated via the DREA web app.

One way to adapt ΔS to the comparison of multiple control or tumor cell lines involves selecting one of the control cell lines as the reference and using that reference to evaluate

the other control cell lines versus tumor cell lines. ΔS could be determined using HFF, for example, as the reference for each control cell line and tumor cell line. The ΔS means of the reference and tumor cell lines would be determined. Then, one can additionally derive the change in the ΔS means of the reference lines against the tumor cell lines ($\Delta\Delta S$). This approach can be used for a group of different control cell lines or similarly applied to replicates of a single control cell line and multiple tumor cell lines. See supplement Figure S1 on $\Delta\Delta S$ for an example.

$$\Delta\Delta S = \Delta S \text{ mean}_{\text{tumor}} - \Delta S \text{ mean}_{\text{control}} \quad (8)$$

3. Results

3.1. Drug Resistance and Sensitivity Focusing Primarily on a Single PNF1 Cell Line

To validate the algorithm, we initially evaluated the effects of selumetinib and other MEK inhibitors on one test cell line. We assessed the ΔS drug sensitivity of ipNF05.5-MX cells (*NF1*^{-/-}) using ipnNF95.11C (*NF1*^{+/-}) as the reference cell line. Using our ΔS measure, we show that these cells are particularly sensitive to PD-0325901 (mirdametininib) and trametinib, and to a lesser extent, selumetinib (Figure 2). In this case, ΔS scores appear to have reasonable concordance with the concentration–response curves. These results agree with clinical trial results, showing significant reductions in plexiform tumor volume after treatment with mirdametininib or trametinib [19–22].

Since ΔS may be considered an alternative to AC50 and AUC-based methods, the Pearson product-moment correlation was used to compare outcomes from ΔS , $\Delta pAC50$, and $\Delta pAUC$ (Figure 2B–D) from three MEK inhibitors (selumetinib, PD-0325901, and trametinib). No strong correlation was found for any pair of endpoints ($\Delta pAC50$ and $\Delta pAUC$, $\Delta pAC50$ and ΔS , $\Delta pAUC$ and ΔS) across all plexiform neurofibroma cell lines. A moderate correlation was found, however, when comparing $\Delta pAC50$ and ΔS for individual cell lines. This outcome could be largely anticipated as those endpoints measure different, albeit interrelated, components of the concentration–response curve (also see Supplemental Table S1). As an extension, no strong correlation was found when monitoring rank outcomes (see Section 3.4—Comparing Ranking Methodologies) from the ΔS mean, $\Delta pAC50$ mean, and $\Delta pAUC$ mean, again suggesting that each endpoint is monitoring a different aspect of the concentration–response curves.

We also note that multiple controls can be used in a single analysis by using Equation (8). See Supplemental Figure S1 for an example.

Individual low-concentration responses higher than 100% of the DMSO control were indicative of drug-stimulated growth, as found for ipNF05.5-MX treated with MEK inhibitors and doxorubicin (Figures 2 and 3). The underlying reason that some drugs display asymptote maximum values above 100% of the DMSO control in Figures 2 and 3 (particularly in ipNF05.5-MX) is not clearly understood. It is possible that these low-concentration responses are due to an unknown experimental variability, or some inherent cell line-to-cell line drug response variability. Supplement Figure S2 compares the histograms of the upper asymptotes from all the plexiform cell lines, including ipNF05.5-MX. All the histograms demonstrated a bell-shaped curve with broadly similar centers. This suggests that it is unlikely that there was a gross plating error or focal cell number error that led to the apparent stimulatory response. It is possible that there is some inherent cell line-to-cell line cause of the low-dose drug response affecting ipNF05.5-MX, which might include hormesis among other explanations.

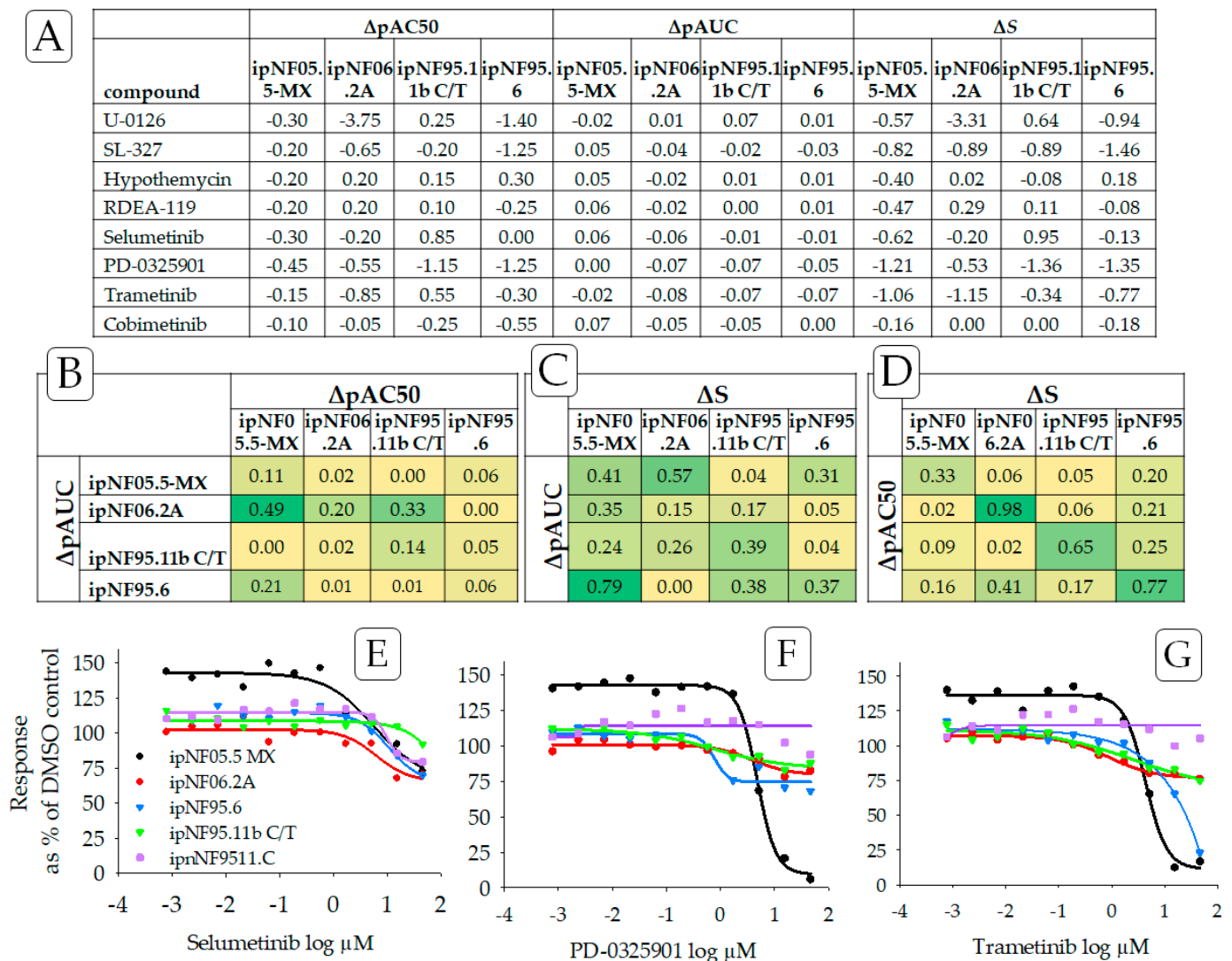


Figure 2. ((A) **Top panel**) Drug sensitivity of the plexiform neurofibroma cell lines to MEK inhibitors, determined using $\Delta pAC50$, $\Delta pAUC$, and ΔS , wherein ipnNF95.11C was used as the reference cell line. We compare ΔS to $\Delta pAC50$ and $\Delta pAUC$, which are frequently used indicators of relative potency. Drug sensitivity responses are negative ΔS values. ((B–D) **Middle panel**) Strength of the relationship of ΔS to $\Delta pAC50$ and $\Delta pAUC$ was examined using the square of Pearson’s product-moment correlation coefficient “ r ” for each pair of cell lines and with color scales applied. The bright green color indicates a high correlation for the relationship, and yellow indicates a low correlation. ((E–G) **Bottom panel**) Also see graphs that illustrate concentration–response curves for three MEK inhibitors showing drug sensitivity: (E) selumetinib, (F) PD-0325901 (mirdametinib), and (G) trametinib. Purple is used to indicate data from the reference non-tumor cell line, ipnNF95.11C. Note how the concentration–response curves that are shifted below the respective reference lines indicate a relative sensitivity for MEK inhibitors.

In contrast to compounds inducing sensitivity, ipNF05.5-MX cells showed resistance to a panel of TOP2A inhibitors, compared to the response of the control ipnNF95.11C cell line (Figure 3). Furthermore, drug resistance was found for 6/7 anthracyclines in ipNF05.5-MX cells. These results were also observed in other PNF1 cell lines when examining the concentration–response curves. Analyses of drugs against a single cell line may be useful when developing precision medicine treatments for tumors that share genetic or proteomic similarities [23].

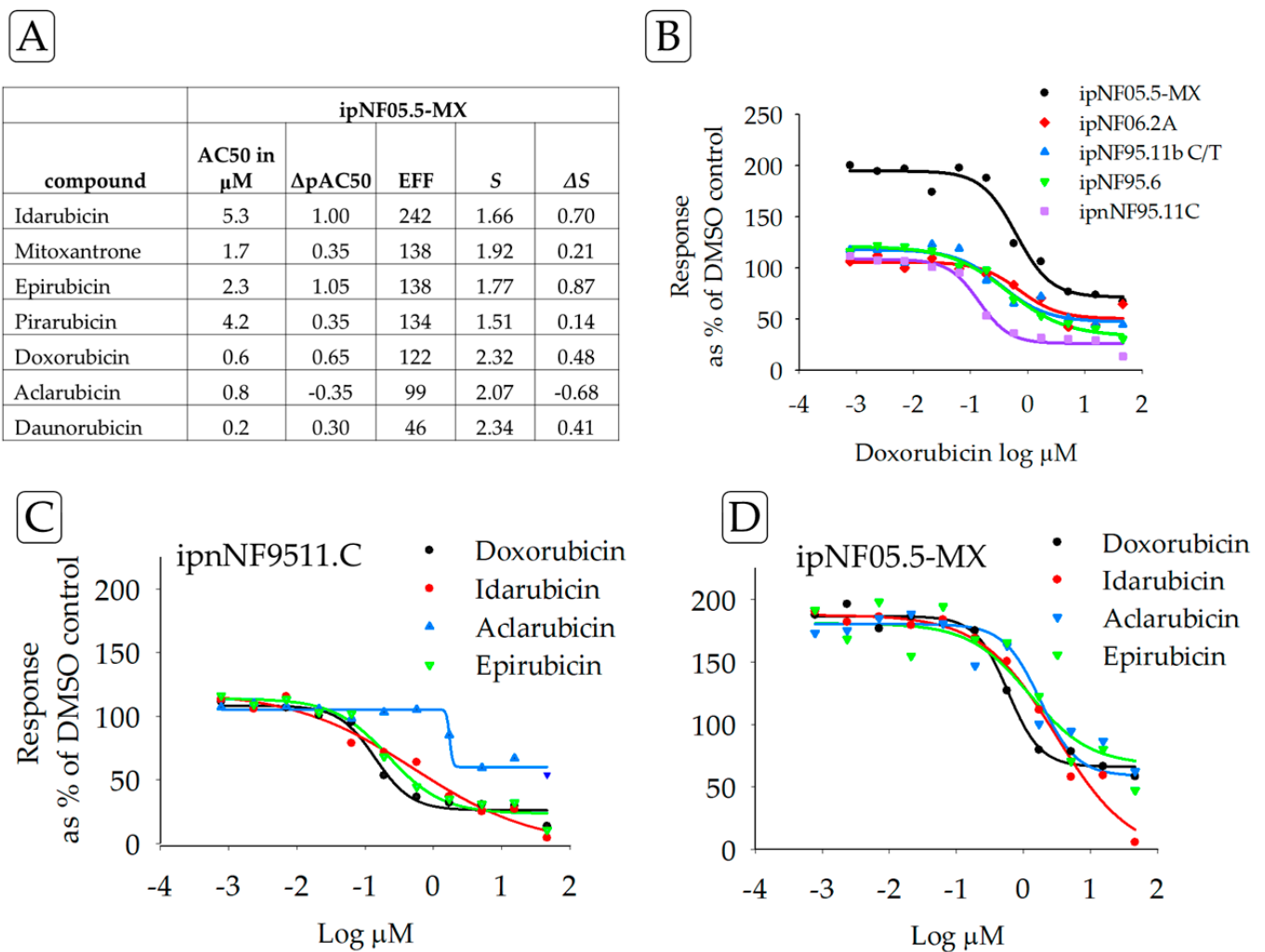


Figure 3. (A) Drug resistance of the ipNF05.5-MX cell line by ΔS for TOP2A inhibitors with ipnNF95.11C as the reference cell line, compared to AC50 and ΔpAC50 , which are frequently used as potency indicators. Drug-resistant responses are positive ΔS values. Using the square of Pearson's product-moment correlation coefficient " r ", a strong correlation was found between ΔS and ΔpAC50 (0.9). (B) The graph illustrates the concentration–response curves for one of the test compounds, doxorubicin, in all the test cell lines. The purple line is the reference, ipnNF95.11C. (C) Concentration–response curves for the reference cell line ipnNF95.11C treated with different TOP2A inhibitors; compared with curves on the right. (D) Concentration–response curves for the plexiform neurofibroma cell line ipNF05.5-MX treated with different TOP2A inhibitors; compared with curves on the left. Collectively, the table and graphs permit a comparison of different parameters for one cell line and the effects of multiple drugs.

3.2. Drug Assessment by Signaling Pathway

In some cases, researchers may want to test whether a molecular signaling pathway as a whole is a promising target for drug discovery. To evaluate drugs across PNF1 cell lines, we used ΔS *mean*, a simple mean of the ΔS values for all four PNF1 cell lines. Table 2 shows the ΔS *mean* for compounds known to affect the PI3K/AKT/MTOR signaling pathway. The top hits in this pathway are GNE-490, triciribine phosphate, and WYE-354, which are known inhibitors of PI3K, AKT, and MTOR, respectively.

Table 2. ΔS drug sensitivity for compounds affecting the PI3K/AKT/mTOR pathway, sorted by the ΔS mean from all four PNF1 cell lines.

PI3KCA			AKT1			MTOR		
Compound	ΔS Mean	ΔS Variance	Compound	ΔS Mean	ΔS Variance	Compound	ΔS Mean	ΔS Variance
GNE-490	−0.66	0.25	Triciribine-PO4	−1.51	0.81	WYE-354	−0.53	1.15
NIBR-17	−0.48	0.14	A-443654	−0.82	0.04	AZD-2014	−0.34	0.24
PIK-90	−0.45	0.01	AT-7867	−0.62	0.16	GDC-0980	−0.24	0.14
BKM-120	−0.33	0.47	AZD-5363	−0.36	0.10	KU-0063794	−0.23	0.04
PF-04691502	−0.31	0.20	GDC-0068	−0.34	0.12	AZD-8055	−0.22	0.38
GNE-493	−0.28	0.08	H-89	−0.26	0.12	WAY-600	−0.20	0.19
PIK-93	−0.28	0.23	MK-2206	−0.13	0.02	PP-242	−0.20	0.89

Additionally, PNF1 tumor cell lines as a group were largely resistant to compounds that target non-RAS-binding partners of neurofibromin [24,25]. Concentration–response curves for two compounds that impact such non-RAS binding partners are found in Figure 4. These binding partners include tubulin [25], HTR6, the focal adhesion protein (FAK) [24,26], and LIMK2 [27]. Here, NVP-TAE226, a FAK inhibitor, and BMS-3, a LIMK1/2 inhibitor, each displayed drug-resistance in PNF1 cell lines.

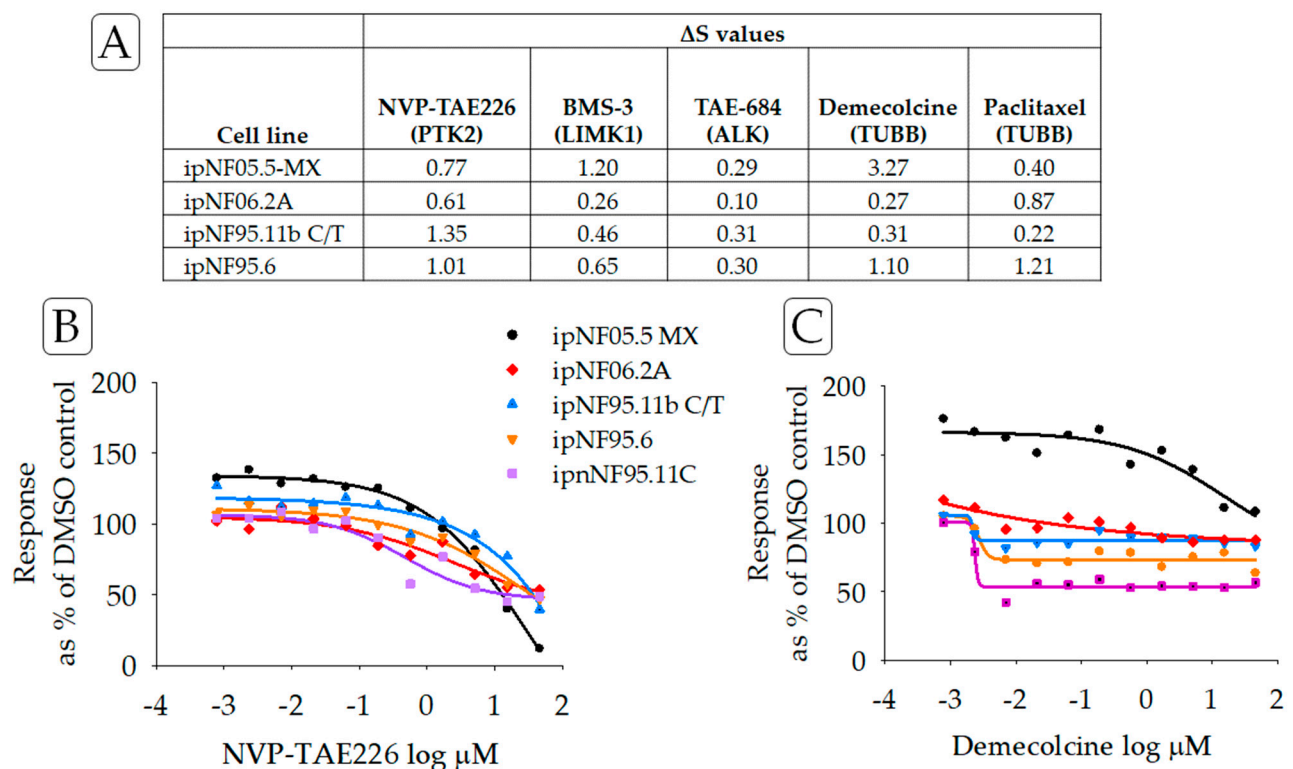


Figure 4. (A) ΔS scores for compounds targeting non-RAS proteins and reportedly binding or associated with neurofibromin. PTK2 (focal adhesion protein, FAK), TUBB (tubulin), LIMK1 (LIM Domain Kinase 1), and ALK (anaplastic lymphoma kinase). (B) Concentration–response curves for NVP-TAE226, an inhibitor of FAK, and (C) demecolcine, an inhibitor of tubulin. Lines in purple indicated data from the reference cell line ipnNF95.11C.

Arranging the results by the ΔS mean score and signaling pathway target may be useful in identifying promising drugs for follow-up (see Table 2). In this regard, AKT inhibitors triciribine phosphate and A-443654 may be of downstream interest.

3.3. Discussion of Prioritized Compounds

In this section, we will discuss a subset of the drugs identified as ‘high-sensitivity’ or ‘resistance’. Analyses of other compounds are detailed in Figures 5 and 6 and can be explored via the DREA web tool (see Supplemental Materials). Prioritized compounds have an average R^2 of at least 0.8 in all four test cell lines and display drug resistance (ΔS mean > 0.5) or drug sensitivity (ΔS mean < -0.5), as described in the methods section. For the current analysis, we compared the response of each cell line (NF1+/–) to that of the ipNF95.11C (NF1+/–) cell line, but responses can also be calculated using several other control lines in DREA.

name of compound	target	ΔS for PNF cell line				ΔS mean	ΔS variance	color code	value
		ipNF05.5 MX	ipNF06.2A	ipNF95.11 b C/T	ipNF95.6				
GSK-2636771	PIK3CB	■	■	■	■	-1.99	0.70	■	-3.5
Triciribine phosphate	AKT1	■	■	■	■	-1.51	0.81	■	-3.0
Clomipramine HCl	SLC6A4	■	■	■	■	-1.35	0.50	■	-2.5
Ketorolac	COX1/2	■	■	■	■	-1.31	0.75	■	-2.0
Sibutramine HCl	HTR1A	■	■	■	■	-1.21	0.27	■	-1.5
Geldanamycin	HSP90AB1	■	■	■	■	-1.20	0.79	■	-1.0
Alvespimycin HCl	HSP90AB1	■	■	■	■	-1.17	0.65	■	-0.5
TAK-285	EGFR	■	■	■	■	-1.12	0.18	■	0.0
Duloxetine HCl	SLC6A4	■	■	■	■	-1.12	0.15	■	0.5
SCH-900776	CHEK1	■	■	■	■	-1.01	0.16	■	
Tivozanib	FLT1	■	■	■	■	-0.95	0.53	■	
Varlitinib tosylate	EGFR	■	■	■	■	-0.92	0.35	■	
Piboserod HCl	HTR4	■	■	■	■	-0.87	0.51	■	
Trametinib	MAP2K1	■	■	■	■	-0.83	0.14	■	
A-443654	AKT1	■	■	■	■	-0.82	0.04	■	
Fluvastatin	HMGCR	■	■	■	■	-0.80	0.04	■	
Mycophenolic acid	IMPDH1	■	■	■	■	-0.77	0.04	■	
R-1487	MAPK14	■	■	■	■	-0.71	0.33	■	
Isradipine	CACNA1E	■	■	■	■	-0.71	0.17	■	
IKK-2 Inhibitor VIII	IKKBK	■	■	■	■	-0.71	0.12	■	
BMS-345541	IKKBK	■	■	■	■	-0.71	0.38	■	
GNE-490	PIK3CA	■	■	■	■	-0.66	0.25	■	
DCC-2036	ABL1	■	■	■	■	-0.64	0.12	■	
AT-7867	AKT1	■	■	■	■	-0.62	0.16	■	
Zosuquidar tri-HCl	ABCBA	■	■	■	■	-0.60	0.09	■	
Retaspimycin	HSP90AB1	■	■	■	■	-0.57	0.18	■	
Mycophenolate mofetil	IMPDH1	■	■	■	■	-0.55	0.06	■	
AIM-100	TNK2	■	■	■	■	-0.54	0.16	■	
Temocapril HCl	ACE	■	■	■	■	-0.53	0.11	■	
Erlotinib HCl	EGFR	■	■	■	■	-0.52	0.21	■	

Figure 5. PNF tumor cell lines displaying drug sensitivity to test compounds meeting the ΔS mean threshold and variance criteria, where all cell lines had data. Red data bars indicate the ΔS for each cell line with lower values (more sensitivity) to the left in each cell. ΔS mean values are arranged from the most sensitive to the least sensitive. A red color indicates compound sensitivity, and blue indicates compound resistance.

name of compound	target	ΔS for PNF cell line				ΔS mean	ΔS variance	color code	value
		ipNF05.5 MX	ipNF06.2A	ipNF95.11 b C/T	ipNF95.6				
Sapitinib	ERBB2	3.5	3.0	2.5	2.0	2.10	1.48	3.5	
Birinapant	XIAP	3.0	2.5	2.0	1.5	1.51	0.40	3.0	
KX-01	SRC	2.5	2.0	1.5	1.0	1.46	0.73	2.5	
Indibutlin	TUBB	2.0	1.5	1.0	0.5	1.44	0.08	2.0	
AST-1306	ERBB2	1.5	1.0	0.5	0.0	1.40	0.30	1.5	
Noscapine	TUBB	1.0	0.5	0.0	-0.5	1.35	0.03	1.0	
PIK-294	PIK3CA	0.5	0.0	-0.5	-1.0	1.27	0.61	0.5	
Gemcitabine	RRM2	0.0	-0.5	-1.0	-1.5	1.09	0.63	0.0	
Idarubicin HCl	TOP2A	-0.5	-1.0	-1.5	-2.0	0.94	0.03	-0.5	
NVP-TAE226	PTK2	-1.0	-1.5	-2.0	-2.5	0.93	0.10	-1.0	
Epirubicin HCl	TOP2A	-1.5	-2.0	-2.5	-3.0	0.90	0.09	-1.5	
Vinflunine	TUBB	-2.0	-2.5	-3.0	-3.5	0.85	0.51	-2.0	
Salinomycin	WNT1	-2.5	-3.0	-3.5	-4.0	0.81	0.34	-2.5	
LY-2874455	FGFR1	-3.0	-3.5	-4.0	-4.5	0.75	0.08	-3.0	
TAK-901	AURKA	-3.5	-4.0	-4.5	-5.0	0.75	0.18	-3.5	
Ixazomib citrate	PSMD1	-4.0	-4.5	-5.0	-5.5	0.71	0.24	-4.0	
AEE-788	EGFR	-4.5	-5.0	-5.5	-6.0	0.69	0.05	-4.5	
Paclitaxel	TUBB	-5.0	-5.5	-6.0	-6.5	0.67	0.20	-5.0	
BMS-3	LIMK1	-5.5	-6.0	-6.5	-7.0	0.64	0.16	-5.5	
Topotecan HCl	TOP1	-6.0	-6.5	-7.0	-7.5	0.62	0.05	-6.0	
Methotrexate	DHFR	-6.5	-7.0	-7.5	-8.0	0.61	0.07	-6.5	
Mitoxantrone	TOP2A	-7.0	-7.5	-8.0	-8.5	0.60	0.08	-7.0	
Doxorubicin	TOP2A	-7.5	-8.0	-8.5	-9.0	0.60	0.05	-7.5	
ARRY-380	ERBB2	-8.0	-8.5	-9.0	-9.5	0.58	0.01	-8.0	
Rabusertib	CHEK1	-8.5	-9.0	-9.5	-10.0	0.56	0.15	-8.5	
ON-01910	PLK1	-9.0	-9.5	-10.0	-10.5	0.55	0.08	-9.0	
BYL-719	PIK3CA	-9.5	-10.0	-10.5	-11.0	0.55	0.16	-9.5	
PF-3758309	PAK4	-10.0	-10.5	-11.0	-11.5	0.54	0.07	-10.0	
NCGC00344999-01	IITK	-10.5	-11.0	-11.5	-12.0	0.54	0.03	-10.5	
G-Strophanthin	NKAIN1	-11.0	-11.5	-12.0	-12.5	0.54	0.23	-11.0	
AHPN	RARG	-11.5	-12.0	-12.5	-13.0	0.53	0.18	-11.5	
Trifluridine	TYMS	-12.0	-12.5	-13.0	-13.5	0.52	0.07	-12.0	
Rifapentine	PRKDC	-12.5	-13.0	-13.5	-14.0	0.51	0.09	-12.5	
XRP-44X	TUBB	-13.0	-13.5	-14.0	-14.5	0.51	0.02	-13.0	
NU-6027	CDK1	-13.5	-14.0	-14.5	-15.0	0.51	0.14	-13.5	

Figure 6. PNF1 tumor cell lines displaying drug-resistance to test compounds meeting the ΔS mean threshold and variance criteria, where all cell lines had data. Blue data bars indicate the ΔS for each cell line with higher values (more resistance) to the right in each cell. Red bars indicate drug sensitivity. ΔS mean values are arranged from the most resistant at the top to the least resistant at the bottom. A red color indicates compound sensitivity, and blue indicates compound resistance.

3.3.1. MEK Inhibitors

Several MEK inhibitors have been used in clinical trials for NF1-related tumors, including the FDA-approved drug selumetinib [7,8]. Our analysis identified trametinib as a prioritized compound, to which PNF1 cell lines as a group were sensitive. Trametinib shows promising results in clinical trials, significantly reducing the neurofibroma tumor size [22,28]. While selumetinib was not prioritized by ΔS mean, some cell lines showed sensitivity to it, suggesting it may be effective in specific tumors or cells therein. In vivo, different neurofibromas, even in the same individual, can carry different somatic NF1 mutations [29]. This can affect both RAS and non-RAS cell responses. Alternatively, the

differences could reflect a more robust compensatory increase in pMEK levels, indicating the occurrence of reactivation of the MAPK pathway [25].

3.3.2. PI3K and AKT1 Inhibitors

The most pronounced drug sensitivity across PNF1 cell lines was to the class I PI3KCB inhibitor GSK-2636771. GSK-2636771 is effective in PTEN-deficient tumors [30,31], presumably compensating for the upregulation of the PI3K/AKT pathway engendered by the loss of PTEN inhibition. PTEN pathway alterations have been implicated in early NF1-associated tumorigenesis [32], with marked PTEN reductions found in MPNSTs compared to both neurofibromas and normal nerve tissue [33,34]. Another PI3K-targeted compound identified in our sensitivity analysis was GNE-490, an experimental, pan-PI3K inhibitor that would be expected to inhibit PI3KCB and PI3KCA [35]. GNE-490 is effective against mouse xenograft models of breast and prostate cancers [35].

In contrast, drug resistance was found for two PI3K inhibitors (see Figure 6): PIK-294, an inhibitor that is somewhat selective for the PI3K catalytic subunit p110 δ [36], and to a lesser extent, BYL-719, which is selective for the p110 α subunit [37]. The result for BYL-719 is unexpected, given the sensitivity of the cells to GNE-490, another p110 α inhibitor. This may suggest differing structure–activity relationships [38] between these compounds and GNE-490 [35].

Acting downstream of PI3K, cell lines were sensitive to three AKT1 inhibitors (tricitriline phosphate, A-443654, and AT-7867). Tricitriline phosphate is the only one of these compounds that has reached the investigational stage of drug development [39]. The identification of AKT-targeting compounds is particularly interesting, given that in MPNSTs neither AKT nor mTORC2 are required for tumor remission [40]. This may reflect important differences in pathway utilization between MPNSTs and PNF1. No AKT-targeting drugs were resistant in our analysis.

3.3.3. TOP2A and CHEK1 Gene Product Inhibitors

TOP2A, one of the top 20 genes upregulated in MPNST [41], encodes the enzyme DNA topoisomerase II alpha, which controls and alters the topologic states of DNA during transcription. Matching this observation, PNF1 tumor cell lines displayed drug-resistance to anthracycline topoisomerase inhibitors, e.g., idarubicin, epirubicin, mitoxantrone, and doxorubicin. Finding anthracycline resistance in PNF1 cell lines suggests that this resistance develops early in the tumorigenesis cascade and may later contribute to the poor therapeutic response of doxorubicin in unresectable MPNSTs [42].

DNA topoisomerase II alpha activates cell cycle progression from the G2 to the M phase by inhibiting CHK1 phosphorylation [43] (CHK1, checkpoint kinase 1, is the protein product of the CHEK1 gene), promoting the epithelial-to-mesenchymal transition and cancer cell invasion. CHK1 is required for checkpoint-mediated cell cycle arrest and is upregulated in MPNST, compared to neurofibromas [44]. We found that cells were sensitive to SCH-900776, which is a selective CHK1 inhibitor. However, these cells were resistant to the CHK1 inhibitor rabusertib. This observation also indicates that there may be an important role in the structure–activity relationships of these compounds and their target. In addition to CHEK1, neurofibromas frequently harbor alterations in PRKDC [45], which may contribute to resistance.

3.3.4. Heat Shock Proteins

We found sensitivity to three drugs targeting HSP90AB1 (geldanamycin, alvespimycin HCl, and retaspimycin). Given that the loss of neurofibromin activates HSF1 to promote carcinogenesis [46], a finding that plexiform neurofibroma cell lines are sensitive to HSP90AB1 inhibitors is not entirely unexpected, and the potential for heat shock protein inhibitors as NF1 treatments has been suggested [47]. Combined treatment with mTOR and HSP90 inhibitors in vitro led to a decrease in LD50 in human and murine MPNST cell lines compared to a human fibroblast cell line (IMR90), and in vivo, to an increase in survival in

tumor-bearing Nf1/p53 mutant mice [48]. While geldanamycin is too toxic to be used clinically, geldanamycin analogs and other HSP90 inhibitors may be good targets for the downstream combination drug evaluation.

3.3.5. Serotonin Modulators

A subset of four prioritized drugs act via serotonin signaling. This is notable in that several antidepressants have carcinostatic effects [49]. Two serotonin reuptake inhibitors (the tricyclic antidepressant clomipramine and the serotonin-noradrenaline reuptake inhibitor duloxetine) were prioritized based on ΔS mean. Clomipramine interferes with autophagic flux in HeLa cells and inhibits growth and “stemness” in lung cancer via its metabolite desmethylclomipramine [50]. Duloxetine is a dual serotonin/norepinephrine reuptake inhibitor that enhances tumor necrosis factor-related apoptosis-inducing ligand (TRAIL) apoptosis in tumor cells [51].

Two serotonin receptor antagonists (piboserod and sibutramine) were also prioritized. Piboserod is a selective antagonist of the G-protein-coupled HTR4 serotonin receptor [52]. Sibutramine, in vivo, is a norepinephrine, serotonin, and dopamine reuptake inhibitor; it has an affinity for several monoaminergic receptors, including HTR1. Both HTR1 and HTR4 can, in some tumor types, act through both the MAPK-ERK pathway and the PI3K-AKT-MTOR pathway [53].

3.3.6. Non-Prioritized Compounds of Interest

We prioritized drug responses that had an average R^2 of at least 0.8 in all four test cell lines and that displayed drug resistance (ΔS mean > 0.5) or drug sensitivity (ΔS mean < -0.5). There were, however, drug responses in the original panel that represented missing values or responses in fewer than four cell lines. Some of the drugs with the highest ΔS mean drug-sensitive scores were not included in the final lists due to a single cell line with missing or inconsistent data. However, these compounds (secoisolaricresinol and verteporfin, for example) may also be of interest in follow-up studies.

3.4. Comparing Ranking Methodologies

Figure 7 provides a relative ranking of test compounds anchored on ΔS means, with comparisons to $\Delta pAC50$ means and $\Delta pAUC$ means. While there were some similarities in rankings, by and large, the rankings across compounds showed little concordance in paired comparisons of $\Delta pAC50$ means, $\Delta pAUC$ means, and ΔS means. This is similar to outcomes found in Figure 2 for $\Delta pAC50$, $\Delta pAUC$, and ΔS . Since these endpoints are derived from the same test system and concentration–response curves, the lack of concordance suggests that $\Delta pAC50$, $\Delta pAUC$, and ΔS measure different aspects of concentration–response curve information.

AC50 and $\Delta pAC50$ are used to monitor changes in drug potency. They do not take into account response effectiveness, which is a second dimension of a concentration–response curve, and can be misleading when comparing drug responses that display full effectiveness to those with partial effectiveness.

The AUC is based on segmenting the entire two-dimensional area underneath the curve and then summing all the sub-values, thereby providing an aggregate measure that considers potency and effectiveness. Differences in the AUC can imply changes in drug sensitivity. Such aggregate values may not always be desirable and may complicate the interpretation of $\Delta pAUC$ because, as pointed out by Guha et al. [13], the AUC for a compound exhibiting a shift in potency but no shift in efficacy can be the same as (or similar to) the AUC for a compound exhibiting a shift in efficacy but not a shift in potency.

The S indices (S and ΔS) incorporate effectiveness and potency and normalize activity through the inclusion of EFF, which is the response effectiveness. This corrects for differences in full or partial drug sensitivity. ΔS can infer the sensitivity (or resistance) of a given drug in a tumor cell line(s) (a proxy for tumors) relative to a reference cell line (a proxy for normal tissue). Compounds with high sensitivity in plexiform neurofibroma cell lines

based on the ΔS or ΔS mean would be good candidates for follow-on confirmatory and/or in vivo studies. It is likely preferable to investigate treatments for non-malignant plexiform neurofibromas, which have high tumor sensitivity relative to normal tissues, as a patient may receive protracted drug treatment.

name	calculated values			rank		
	$\Delta pAC50$ mean	$\Delta pAUC$ mean	ΔS mean	$\Delta pAC50$ mean	$\Delta pAUC$ mean	ΔS mean
GSK-2636771	-1.29	-0.11	-1.99	3	1	1
Triciribine phosphate	-0.84	-0.05	-1.51	10	6	2
Clomipramine HCl	-0.74	-0.01	-1.35	12	12	3
Ketorolac	-0.49	0.03	-1.31	14	19	4
Sibutramine HCl	-0.96	-0.11	-1.21	8	2	5
Geldanamycin	-0.36	-0.05	-1.20	18	8	6
Alvespimycin HCl	-0.59	-0.01	-1.17	14	13	7
TAK-285	-0.91	0.01	-1.12	9	16	8
Duloxetine HCl	-1.10	-0.05	-1.12	4	9	9
SCH-900776	-1.50	0.00	-1.01	2	14	10
Tivozanib	-1.04	0.01	-0.95	5	17	11
Varlitinib tosylate	-0.41	-0.02	-0.92	17	11	12
Piboserod HCl	-0.11	0.01	-0.87	20	18	13
Trametinib	-0.99	0.01	-0.83	7	15	14
A-443654	-1.00	-0.10	-0.82	6	3	15
Fluvastatin	-0.42	-0.05	-0.80	16	7	16
Mycophenolic acid	-0.19	-0.06	-0.77	19	5	17
R-1487	-1.71	-0.07	-0.71	1	4	18
Isradipine	-0.79	-0.03	-0.71	11	10	19
IKK-2 Inhibitor VIII	-0.66	0.06	-0.71	13	20	20

Figure 7. Comparison of $\Delta pAC50$ mean, $\Delta pAUC$ mean, and ΔS mean scores from plexiform neurofibroma cell lines. The cell line ipnNF9511.C derived from the non-tumor nerve was used as the reference in the calculations. Outcomes for ΔS mean (see Figure 5) are ranked and color-coded to facilitate comparison, and the rank is compared to that derived from the $\Delta pAC50$ mean and $\Delta pAUC$ mean. Bright yellow indicates the top ranking for each column/calculation method and dark blue indicates the bottom ranking.

4. Conclusions

In this study, AC50 and EFF were combined into a single value (S) to furnish system-independent ratios (ΔS and ΔS mean), used to assess the relative drug sensitivity and drug resistance of a panel of compounds. The combination of EFF and AC50 into a single value considers the heterogeneous effects of partial and full drug responses. Using our algorithm, we recapitulate the identification of MEK inhibitors as potential therapeutics for NF1-related tumors and identify other compounds to which PNF1 cell lines are particularly sensitive or resistant. We suggest that the algorithms behind the Drug Response Evaluation and Assessment (DREA) web tool (available at: <https://nf.mocomakers.com>) can also be used in both primary cell cultures and other cell models, including induced pluripotent stem cells (iPSCs) [54]. Given high-throughput data, the algorithm can be applied to any

cancer model as needed. For example, the used dataset [15] had other cell lines, such as human foreskin fibroblasts (HFFs) that may be useful in other styles of analysis.

Compounds with partial or low efficacy can represent important modulators of biological activity and may be particularly difficult to recognize based on AC50 analysis only. The use of ΔS may help to identify promising compounds that display partial effectiveness. The use of ΔS *mean* outcomes from multiple cell lines, as used here, may help in addressing drugs that generate partial responses in vitro and help address the known heterogeneity found in tumor cells and tumor cell lines in general [55–57]. DREA can be used to assess candidate compounds individually by the cell line, as in Figures 5 and 6. This allows an analysis to reflect the molecular heterogeneity of different cell lines. In the development of treatments, wide applicability of the treatment is vital. Therefore, we also assess the ΔS *mean* and variance values, reflecting responses of PNF1 cell lines as a group, with the goal of assuring biological relevance and approaching response uniformity across PNF1 cell lines.

The current study focused on the use of single agent screens; however, it is possible that the S indices could be useful to guide the examination of drug combinations using a modification of the IDACombo method [58] and/or SynergyFinder 3.0 [59]. IDACombo is based on independent drug action (IDA), where the therapeutic benefit is derived from the single most effective drug in a drug combination. SynergyFinder 3.0 incorporates a parametric synergy scoring model and multi-dimensional synergy of combinations (MuSyC), which provides the users with the possibility to distinguish whether the identified synergy is due to enhanced potency and/or efficacy of the single agents.

The use of S indices, particularly ΔS *mean* when data are available for multiple cell lines with a common reference line, can be useful in the high-throughput screening assessment of potentially therapeutical useful compounds for the treatment of NF1-related tumors and other cancers. When prioritizing research for a rare disease such as NF1, a cross-compound analysis such as this may be of utility for focusing on the promising mechanisms of action, as well as investigational therapeutics. Our results provide both an affirmation of already approved or developing therapeutics, but also serve as the basis for further pre-clinical evaluations of high-scoring but sparsely explored compounds.

It is also essential to increase to robustness of our method to incorporate multiple control cell lines within the analysis when possible. In this analysis, we used a limited dataset of plexiform neurofibroma cell lines, precluding the use of multiple controls in the current work. However, in fields like breast cancer, where there are more known control lines, an $\Delta\Delta S$ analysis with multiple controls could likely be done.

It is envisioned that ΔS could be used as part of an overall orthogonal approach to drug evaluation and selection. Orthogonal approaches combined with ΔS could help increase the predictive value of in vitro concentration–response studies and, thereby, reduce the cost and time constraints of follow-on in vivo studies and pre-clinical drug development. With an orthogonal approach, ΔS may also be able to provide a different perspective, if not clarity, on known issues related to the individual use of AC50, effectiveness, or AUC.

Supplementary Materials: The following supporting information can be downloaded at: <https://www.mdpi.com/article/10.3390/cancers15245811/s1>, Table S1: Simulated effect of changing EFF and AC50 for a number of model compounds; Figure S1: $\Delta\Delta S$ outcomes from a series of compounds targeting MEK, and targeting JAK2; Figure S2: Histogram of maximum (upper) asymptotes for all tested compounds by target plexiform neurofibroma cell line. An exploratory Drug Response Evaluation and Assessment (DREA) Web Tool was developed in the Python programming language for our methods. This tool can be accessed at <https://nf.mocomakers.com> and it includes data visualizations, our derived fields, as well as additional filters and cell lines for expanded investigation potential. For more tips on using this tool, please see: https://github.com/MoCoMakers/nf_streamlit/wiki.

Author Contributions: Conceptualization, P.O.Z., M.Z. and G.A.; methodology, P.O.Z. and G.A.; software, M.Z. and G.A.; validation, P.O.Z., M.Z. and G.A.; formal analysis, G.A.; investigation, P.O.Z., M.Z., G.A., N.D., H.D. and C.I.M.; resources, U.S.; data curation, G.A.; writing—original draft preparation, P.O.Z. and D.B.; writing—review and editing, D.B.; visualization, D.B.; supervision, U.S.; project administration, M.Z.; funding acquisition, M.Z. and U.S. All authors have read and agreed to the published version of the manuscript.

Funding: The authors acknowledge the Children’s Tumor Foundation for financial support as part of the incubation prize for the 2022 Hack4NF community challenge series. The CTF group is empowering the growth of the NF research community and driving the industry toward finding a cure.

Informed Consent Statement: Not applicable.

Data Availability Statement: In the provided Supplementary Material. This tool and our algorithm are available on https://github.com/MoCoMakers/nf_streamlit/ (accessed on 8 September 2023). Quantitative High-Throughput Screening data are available for the MIPE4.0 library of small molecules from <https://www.synapse.org/#!/Synapse:syn5522627> (accessed on 1 May 2023).

Acknowledgments: The authors acknowledge the MoCo Maker technology and scientific education community, whose many members contributed to this project. DMV Petri Dish contributed their membership and knowledge in bioinformatics and broader biological science topics. The HacDC group contributed their technical expertise, which would amaze most scientists. All contributors to Team MCH—winners of the 2022 Hack4NF competition—are strongly acknowledged. While there are too many to list, we particularly thank Aastha Naik, Antony Haider, Varun Srinivasan, Chuba Oraka, and Brikena Kay. Additionally, we strongly appreciate Richard Conroy and the Capital Area Biospace community for helping us spearhead this project and for helping our group attend CTF’s NF Conference in Phoenix 2023 to present early versions of our work.

Conflicts of Interest: Authors Paul O. Zamora, Nathan Dwarshuis, Hari Donthi and Matthew Zamora were employed by the company MoCo Makers. Author Gabriel Altay was employed by the company HacDC. Author Ulisses Santamaria was employed by the company DMV Petri Dish. The remaining authors declare that the research was conducted in the absence of any commercial or financial relationships that could be construed as a potential conflict of interest.

References

1. Ballester, R.; Marchuk, D.; Boguski, M.; Saulino, A.; Letcher, R.; Wigler, M.; Collins, F. The NF1 locus encodes a protein functionally related to mammalian GAP and yeast IRA proteins. *Cell* **1990**, *63*, 851–859. [[CrossRef](#)] [[PubMed](#)]
2. Martin, G.A.; Viskochil, D.; Bollag, G.; McCabe, P.C.; Crosier, W.J.; Haubruck, H.; Conroy, L.; Clark, R.; O’Connell, P.; Cawthon, R.M.; et al. The GAP-related domain of the neurofibromatosis type 1 gene product interacts with ras p21. *Cell* **1990**, *63*, 843–849. [[CrossRef](#)] [[PubMed](#)]
3. Evans, D.G.; Baser, M.E.; McGaughran, J.; Sharif, S.; Howard, E.; Moran, A. Malignant peripheral nerve sheath tumours in neurofibromatosis 1. *J. Med. Genet.* **2002**, *39*, 311–314. [[CrossRef](#)] [[PubMed](#)]
4. Uusitalo, E.; Leppavirta, J.; Koffert, A.; Suominen, S.; Vahtera, J.; Vahlberg, T.; Poyhonen, M.; Peltonen, J.; Peltonen, S. Incidence and mortality of neurofibromatosis: A total population study in Finland. *J. Invest. Dermatol.* **2015**, *135*, 904–906. [[CrossRef](#)] [[PubMed](#)]
5. Somatilaka, B.N.; Sadek, A.; McKay, R.M.; Le, L.Q. Malignant peripheral nerve sheath tumor: Models, biology, and translation. *Oncogene* **2022**, *41*, 2405–2421. [[CrossRef](#)]
6. Dombi, E.; Baldwin, A.; Marcus, L.J.; Fisher, M.J.; Weiss, B.; Kim, A.; Whitcomb, P.; Martin, S.; Aschbacher-Smith, L.E.; Rizvi, T.A.; et al. Activity of Selumetinib in Neurofibromatosis Type 1-Related Plexiform Neurofibromas. *N. Engl. J. Med.* **2016**, *375*, 2550–2560. [[CrossRef](#)] [[PubMed](#)]
7. Gross, A.M.; Dombi, E.; Wolters, P.L.; Baldwin, A.; Dufek, A.; Herrera, K.; Martin, S.; Derdak, J.; Heisey, K.S.; Whitcomb, P.M.; et al. Long-Term Safety and Efficacy of Selumetinib in Children with Neurofibromatosis Type 1 on a Phase 1/2 Trial for Inoperable Plexiform Neurofibromas. *Neuro Oncol.* **2023**, *25*, 1883–1894. [[CrossRef](#)] [[PubMed](#)]
8. Gross, A.M.; Wolters, P.L.; Dombi, E.; Baldwin, A.; Whitcomb, P.; Fisher, M.J.; Weiss, B.; Kim, A.; Bornhorst, M.; Shah, A.C.; et al. Selumetinib in Children with Inoperable Plexiform Neurofibromas. *N. Engl. J. Med.* **2020**, *382*, 1430–1442. [[CrossRef](#)]
9. Inglese, J.; Auld, D.S.; Jadhav, A.; Johnson, R.L.; Simeonov, A.; Yasgar, A.; Zheng, W.; Austin, C.P. Quantitative high-throughput screening: A titration-based approach that efficiently identifies biological activities in large chemical libraries. *Proc. Natl. Acad. Sci. USA* **2006**, *103*, 11473–11478. [[CrossRef](#)]
10. Kenakin, T. A Scale of Agonism and Allosteric Modulation for Assessment of Selectivity, Bias, and Receptor Mutation. *Mol. Pharmacol.* **2017**, *92*, 414–424. [[CrossRef](#)]

11. Fallahi-Sichani, M.; Honarnejad, S.; Heiser, L.M.; Gray, J.W.; Sorger, P.K. Metrics other than potency reveal systematic variation in responses to cancer drugs. *Nat. Chem. Biol.* **2013**, *9*, 708–714. [[CrossRef](#)] [[PubMed](#)]
12. Shockley, K.R.; Gupta, S.; Harris, S.F.; Lahiri, S.N.; Peddada, S.D. Quality Control of Quantitative High Throughput Screening Data. *Front. Genet.* **2019**, *10*, 387. [[CrossRef](#)]
13. Guha, R.; Mathews Griner, L.A.; Keller, J.M.; Zhang, X.; Fitzgerald, D.; Antignani, A.; Pastan, I.; Thomas, C.J.; Ferrer, M. Ranking Differential Drug Activities from Dose-Response Synthetic Lethality Screens. *J. Biomol. Screen.* **2016**, *21*, 942–955. [[CrossRef](#)] [[PubMed](#)]
14. Winpenny, D.; Clark, M.; Cawkill, D. Biased ligand quantification in drug discovery: From theory to high throughput screening to identify new biased mu opioid receptor agonists. *Br. J. Pharmacol.* **2016**, *173*, 1393–1403. [[CrossRef](#)] [[PubMed](#)]
15. Ferrer, M.; Gosline, S.J.C.; Stathis, M.; Zhang, X.; Guo, X.; Guha, R.; Ryman, D.A.; Wallace, M.R.; Kasch-Semenza, L.; Hao, H.; et al. Pharmacological and genomic profiling of neurofibromatosis type 1 plexiform neurofibroma-derived schwann cells. *Sci. Data* **2018**, *5*, 180106. [[CrossRef](#)]
16. Li, H.; Chang, L.J.; Neubauer, D.R.; Muir, D.F.; Wallace, M.R. Immortalization of human normal and NF1 neurofibroma Schwann cells. *Lab. Invest.* **2016**, *96*, 1105–1115. [[CrossRef](#)]
17. Mathews Griner, L.A.; Guha, R.; Shinn, P.; Young, R.M.; Keller, J.M.; Liu, D.; Goldlust, I.S.; Yasgar, A.; McKnight, C.; Boxer, M.B.; et al. High-throughput combinatorial screening identifies drugs that cooperate with ibrutinib to kill activated B-cell-like diffuse large B-cell lymphoma cells. *Proc. Natl. Acad. Sci. USA* **2014**, *111*, 2349–2354. [[CrossRef](#)]
18. Ehlert, F.J.; Griffin, M.T.; Sawyer, G.W.; Bailon, R. A simple method for estimation of agonist activity at receptor subtypes: Comparison of native and cloned M3 muscarinic receptors in guinea pig ileum and transfected cells. *J. Pharmacol. Exp. Ther.* **1999**, *289*, 981–992.
19. Weiss, B.; Plotkin, S.; Widemann, B.; Tonsgard, J.; Blakeley, J.; Allen, J.; Schorry, E.; Korf, B.; Rosser, T.; Goldman, S.; et al. NFM-06. NF106: Phase 2 Trial of The mek inhibitor PD-0325901 in adolescents and adults with NF1-related plexiform neurofibromas: An nf clinical trials consortium study. *Neuro Oncol.* **2018**, *20*, i143. [[CrossRef](#)]
20. Weiss, B.D.; Wolters, P.L.; Plotkin, S.R.; Widemann, B.C.; Tonsgard, J.H.; Blakeley, J.; Allen, J.C.; Schorry, E.; Korf, B.; Robison, N.J.; et al. NF106: A Neurofibromatosis Clinical Trials Consortium Phase II Trial of the MEK Inhibitor Mirdametinib (PD-0325901) in Adolescents and Adults with NF1-Related Plexiform Neurofibromas. *J. Clin. Oncol.* **2021**, *39*, 797–806. [[CrossRef](#)]
21. Perreault, S.; Larouche, V.; Tabori, U.; Hawkin, C.; Lippe, S.; Ellezam, B.; Decarie, J.C.; Theoret, Y.; Metras, M.E.; Sultan, S.; et al. A phase 2 study of trametinib for patients with pediatric glioma or plexiform neurofibroma with refractory tumor and activation of the MAPK/ERK pathway: TRAM-01. *BMC Cancer* **2019**, *19*, 1250. [[CrossRef](#)] [[PubMed](#)]
22. McCowage, G.B.; Mueller, S.; Pratilas, C.A.; Hargrave, D.R.; Moertel, C.L.; Whitlock, J.; Fox, E.; Hingorani, P.; Russo, M.W.; Dasgupta, K.; et al. Trametinib in pediatric patients with neurofibromatosis type 1 (NF-1)-associated plexiform neurofibroma: A phase I/IIa study. *J. Clin. Oncol.* **2018**, *36*, 10504. [[CrossRef](#)]
23. Krzyszczyk, P.; Acevedo, A.; Davidoff, E.J.; Timmins, L.M.; Marrero-Berrios, I.; Patel, M.; White, C.; Lowe, C.; Sherba, J.J.; Hartmanshenn, C.; et al. The growing role of precision and personalized medicine for cancer treatment. *Technol. Singap. World Sci.* **2018**, *6*, 79–100. [[CrossRef](#)] [[PubMed](#)]
24. Bergoug, M.; Doudeau, M.; Godin, F.; Mosrin, C.; Vallee, B.; Benedetti, H. Neurofibromin Structure, Functions and Regulation. *Cells* **2020**, *9*, 2365. [[CrossRef](#)] [[PubMed](#)]
25. Baez-Flores, J.; Rodriguez-Martin, M.; Lcal, J. The therapeutic potential of neurofibromin signaling pathways and binding partners. *Commun. Biol.* **2023**, *6*, 436. [[CrossRef](#)]
26. Kweh, F.; Zheng, M.; Kurenova, E.; Wallace, M.; Golubovskaya, V.; Cance, W.G. Neurofibromin physically interacts with the N-terminal domain of focal adhesion kinase. *Mol. Carcinog.* **2009**, *48*, 1005–1017. [[CrossRef](#)]
27. Vallee, B.; Doudeau, M.; Godin, F.; Gombault, A.; Tchalikian, A.; de Tauzia, M.L.; Benedetti, H. Nf1 RasGAP inhibition of LIMK2 mediates a new cross-talk between Ras and Rho pathways. *PLoS ONE* **2012**, *7*, e47283. [[CrossRef](#)]
28. Wang, D.; Ge, L.; Guo, Z.; Li, Y.; Zhu, B.; Wang, W.; Wei, C.; Li, Q.; Wang, Z. Efficacy and Safety of Trametinib in Neurofibromatosis Type 1-Associated Plexiform Neurofibroma and Low-Grade Glioma: A Systematic Review and Meta-Analysis. *Pharmaceuticals* **2022**, *15*, 956. [[CrossRef](#)]
29. Thomas, L.; Spurlock, G.; Eudall, C.; Thomas, N.S.; Mort, M.; Hamby, S.E.; Chuzhanova, N.; Brems, H.; Legius, E.; Cooper, D.N.; et al. Exploring the somatic NF1 mutational spectrum associated with NF1 cutaneous neurofibromas. *Eur. J. Hum. Genet.* **2012**, *20*, 411–419. [[CrossRef](#)]
30. Sarker, D.; Dawson, N.A.; Aparicio, A.M.; Dorff, T.B.; Pantuck, A.J.; Vaishampayan, U.N.; Henson, L.; Vasist, L.; Roy-Ghanta, S.; Gorczyca, M.; et al. A Phase I, Open-Label, Dose-Finding Study of GSK2636771, a PI3Kbeta Inhibitor, Administered with Enzalutamide in Patients with Metastatic Castration-Resistant Prostate Cancer. *Clin. Cancer Res.* **2021**, *27*, 5248–5257. [[CrossRef](#)]
31. Mateo, J.; Ganji, G.; Lemech, C.; Burris, H.A.; Han, S.W.; Swales, K.; Decordova, S.; DeYoung, M.P.; Smith, D.A.; Kalyana-Sundaram, S.; et al. A First-Time-in-Human Study of GSK2636771, a Phosphoinositide 3 Kinase Beta-Selective Inhibitor, in Patients with Advanced Solid Tumors. *Clin. Cancer Res.* **2017**, *23*, 5981–5992. [[CrossRef](#)]
32. Gregorian, C.; Nakashima, J.; Dry, S.M.; Nghiemphu, P.L.; Smith, K.B.; Ao, Y.; Dang, J.; Lawson, G.; Mellinghoff, I.K.; Mischel, P.S.; et al. PTEN dosage is essential for neurofibroma development and malignant transformation. *Proc. Natl. Acad. Sci. USA* **2009**, *106*, 19479–19484. [[CrossRef](#)] [[PubMed](#)]

33. Bradtmoller, M.; Hartmann, C.; Zietsch, J.; Jaschke, S.; Mautner, V.F.; Kurtz, A.; Park, S.J.; Baier, M.; Harder, A.; Reuss, D.; et al. Impaired Pten expression in human malignant peripheral nerve sheath tumours. *PLoS ONE* **2012**, *7*, e47595. [[CrossRef](#)] [[PubMed](#)]
34. Pemov, A.; Li, H.; Presley, W.; Wallace, M.R.; Miller, D.T. Genetics of human malignant peripheral nerve sheath tumors. *Neurooncol. Adv.* **2020**, *2*, i50–i61. [[CrossRef](#)]
35. Sutherlin, D.P.; Sampath, D.; Berry, M.; Castanedo, G.; Chang, Z.; Chuckowree, I.; Dotson, J.; Folkes, A.; Friedman, L.; Goldsmith, R.; et al. Discovery of (thienopyrimidin-2-yl)aminopyrimidines as potent, selective, and orally available pan-PI3-kinase and dual pan-PI3-kinase/mTOR inhibitors for the treatment of cancer. *J. Med. Chem.* **2010**, *53*, 1086–1097. [[CrossRef](#)] [[PubMed](#)]
36. Setti, A.; Kumar, M.J.; Babu, K.R.; Rasagna, A.; Prasanna, M.G.; Devi, T.A.; Pawar, S.C. Potency and pharmacokinetics of broad spectrum and isoform-specific p110gamma and delta inhibitors in cancers. *J. Recept. Signal Transduct. Res.* **2016**, *36*, 26–36. [[CrossRef](#)]
37. Wong, C.H.; Ma, B.B.; Cheong, H.T.; Hui, C.W.; Hui, E.P.; Chan, A.T. Preclinical evaluation of PI3K inhibitor BYL719 as a single agent and its synergism in combination with cisplatin or MEK inhibitor in nasopharyngeal carcinoma (NPC). *Am. J. Cancer Res.* **2015**, *5*, 1496–1506.
38. Guha, R. On exploring structure-activity relationships. *Methods Mol. Biol.* **2013**, *993*, 81–94. [[CrossRef](#)]
39. Garrett, C.R.; Coppola, D.; Wenham, R.M.; Cubitt, C.L.; Neuger, A.M.; Frost, T.J.; Lush, R.M.; Sullivan, D.M.; Cheng, J.Q.; Sebti, S.M. Phase I pharmacokinetic and pharmacodynamic study of triciribine phosphate monohydrate, a small-molecule inhibitor of AKT phosphorylation, in adult subjects with solid tumors containing activated AKT. *Investig. New Drugs* **2011**, *29*, 1381–1389. [[CrossRef](#)]
40. Malone, C.F.; Fromm, J.A.; Maertens, O.; DeRaedt, T.; Ingraham, R.; Cichowski, K. Defining key signaling nodes and therapeutic biomarkers in NF1-mutant cancers. *Cancer Discov.* **2014**, *4*, 1062–1073. [[CrossRef](#)]
41. Martinez, M.; Sorzano, C.O.S.; Pascual-Montano, A.; Carazo, J.M. Gene signature associated with benign neurofibroma transformation to malignant peripheral nerve sheath tumors. *PLoS ONE* **2017**, *12*, e0178316. [[CrossRef](#)] [[PubMed](#)]
42. Prudner, B.C.; Ball, T.; Rathore, R.; Hirbe, A.C. Diagnosis and management of malignant peripheral nerve sheath tumors: Current practice and future perspectives. *Neurooncol. Adv.* **2020**, *2*, i40–i49. [[CrossRef](#)]
43. Wang, T.; Lu, J.; Wang, R.; Cao, W.; Xu, J. TOP2A promotes proliferation and metastasis of hepatocellular carcinoma regulated by miR-144-3p. *J. Cancer* **2022**, *13*, 589–601. [[CrossRef](#)] [[PubMed](#)]
44. Stricker, T.P.; Henriksen, K.J.; Tonsgard, J.H.; Montag, A.G.; Krausz, T.N.; Pytel, P. Expression profiling of 519 kinase genes in matched malignant peripheral nerve sheath tumor/plexiform neurofibroma samples is discriminatory and identifies mitotic regulators BUB1B, PBK and NEK2 as overexpressed with transformation. *Mod. Pathol.* **2013**, *26*, 930–943. [[CrossRef](#)] [[PubMed](#)]
45. Consortium, A.P.G. AACR Project GENIE: Powering Precision Medicine through an International Consortium. *Cancer Discov.* **2017**, *7*, 818–831. [[CrossRef](#)]
46. Dai, C.; Santagata, S.; Tang, Z.; Shi, J.; Cao, J.; Kwon, H.; Bronson, R.T.; Whitesell, L.; Lindquist, S. Loss of tumor suppressor NF1 activates HSF1 to promote carcinogenesis. *J. Clin. Investig.* **2012**, *122*, 3742–3754. [[CrossRef](#)]
47. Vitte, J.; Giovannini, M. Potential of HSP90 Inhibitors to Treat Neurofibromatosis-Related Tumors. In *Heat Shock Protein-Based Therapies*; Asea, A.A.A., Almasoud, N.N., Krishnan, S., Kaur, P., Eds.; Springer: Cham, Switzerland, 2015. [[CrossRef](#)]
48. De Raedt, T.; Walton, Z.; Yecies, J.L.; Li, D.; Chen, Y.; Malone, C.F.; Maertens, O.; Jeong, S.M.; Bronson, R.T.; Lebleu, V.; et al. Exploiting cancer cell vulnerabilities to develop a combination therapy for ras-driven tumors. *Cancer Cell* **2011**, *20*, 400–413. [[CrossRef](#)]
49. Zheng, Y.; Chang, X.; Huang, Y.; He, D. The application of antidepressant drugs in cancer treatment. *Biomed. Pharmacother.* **2023**, *157*, 113985. [[CrossRef](#)]
50. Rossi, M.; Munarriz, E.R.; Bartesaghi, S.; Milanese, M.; Dinsdale, D.; Guerra-Martin, M.A.; Bampton, E.T.; Glynn, P.; Bonanno, G.; Knight, R.A.; et al. Desmethylclomipramine induces the accumulation of autophagy markers by blocking autophagic flux. *J. Cell Sci.* **2009**, *122*, 3330–3339. [[CrossRef](#)]
51. Zinnah, K.M.A.; Park, S.Y. Duloxetine Enhances TRAIL-mediated Apoptosis via AMPK-mediated Inhibition of Autophagy Flux in Lung Cancer Cells. *Anticancer. Res.* **2019**, *39*, 6621–6633. [[CrossRef](#)]
52. Sangkuhl, K.; Klein, T.E.; Altman, R.B. Selective serotonin reuptake inhibitors pathway. *Pharmacogenet. Genom.* **2009**, *19*, 907–909. [[CrossRef](#)] [[PubMed](#)]
53. Karmakar, S.; Lal, G. Role of serotonin receptor signaling in cancer cells and anti-tumor immunity. *Theranostics* **2021**, *11*, 5296–5312. [[CrossRef](#)] [[PubMed](#)]
54. Mazuelas, H.; Magallon-Lorenz, M.; Fernandez-Rodriguez, J.; Uriarte-Arrazola, I.; Richaud-Patin, Y.; Terribas, E.; Villanueva, A.; Castellanos, E.; Blanco, I.; Raya, A.; et al. Modeling iPSC-derived human neurofibroma-like tumors in mice uncovers the heterogeneity of Schwann cells within plexiform neurofibromas. *Cell Rep.* **2022**, *38*, 110385. [[CrossRef](#)] [[PubMed](#)]
55. Watson, M.A.; Perry, A.; Tihan, T.; Prayson, R.A.; Guha, A.; Bridge, J.; Ferner, R.; Gutmann, D.H. Gene expression profiling reveals unique molecular subtypes of Neurofibromatosis Type I-associated and sporadic malignant peripheral nerve sheath tumors. *Brain Pathol.* **2004**, *14*, 297–303. [[CrossRef](#)]
56. Thomas, L.; Mautner, V.F.; Cooper, D.N.; Upadhyaya, M. Molecular heterogeneity in malignant peripheral nerve sheath tumors associated with neurofibromatosis type 1. *Hum. Genom.* **2012**, *6*, 18. [[CrossRef](#)]
57. Tyner, J.W.; Haderk, F.; Kumaraswamy, A.; Baughn, L.B.; Van Ness, B.; Liu, S.; Marathe, H.; Alumkal, J.J.; Bivona, T.G.; Chan, K.S.; et al. Understanding Drug Sensitivity and Tackling Resistance in Cancer. *Cancer Res.* **2022**, *82*, 1448–1460. [[CrossRef](#)]

58. Ling, A.; Huang, R.S. Computationally predicting clinical drug combination efficacy with cancer cell line screens and independent drug action. *Nat. Commun.* **2020**, *11*, 5848. [[CrossRef](#)]
59. Ianevski, A.; Giri, A.K.; Aittokallio, T. SynergyFinder 3.0: An interactive analysis and consensus interpretation of multi-drug synergies across multiple samples. *Nucleic Acids Res.* **2022**, *50*, W739–W743. [[CrossRef](#)]

Disclaimer/Publisher’s Note: The statements, opinions and data contained in all publications are solely those of the individual author(s) and contributor(s) and not of MDPI and/or the editor(s). MDPI and/or the editor(s) disclaim responsibility for any injury to people or property resulting from any ideas, methods, instructions or products referred to in the content.